Electronic Supplementary Information (ESI)

for

Dioxygen Reactivity of Iron(II)-Gentisate/1,4-Dihydroxy-2-naphthoate Complexes of N4 Ligands: Oxidative Coupling of 1,4-Dihydroxy-2-naphthoate

Rubina Rahaman,[a,b] *Sandip Munshi,*[a] *Sridhar Banerjee,*[a] *Biswarup Chakraborty,*[a] *Sarmistha Bhunia,*[a] *and Tapan Kanti Paine*[a,]*

[a]School of Chemical Sciences, Indian Association for the Cultivation of Science,

2A & 2B Raja S. C. Mullick Road, Jadavpur, Kolkata-700032, India.

[b]Present Address: Department of Chemistry, Krishnagar Government College,

Krishnagar, West Bengal-741101, India.

Table S1. Crystallographic data for **1**, **3a**, **1**$^{\mathbf{Ox}}$, **2**$^{\mathbf{Ox}}$ and **2F**.

Compound	**1**$\cdot\mathbf{CH_2Cl_2}$ $\cdot\mathbf{C_4H_{10}O}$	**3a**	**1**$^{\mathbf{Ox}}$	**2**$^{\mathbf{Ox}}$	**2F**
Empirical formula	$C_{57}H_{61}BCl_2FeN_4O_5$	$C_{35}H_{25}FeClN_7O_8$	$C_{42}H_{32}FeN_4O_7$	$C_{38}H_{30}FeN_4O_8$	$C_{21}H_{10}O_6$
Formula weight	1019.66	762.92	760.56	726.51	358.29
Crystal system	monoclinic	triclinic	triclinic	triclinic	monoclinic
Space group	*P2(1)/n*	*P -1*	*P -1*	*P -1*	*P21/c*
a, Å	20.700(3)	13.220(19)	9.0769(15)	9.834(5)	4.7327(17)
b, Å	9.7342(14)	14.16(2)	11.7420(19)	11.435(6)	22.284(8)
c, Å	26.459(4)	14.36(2)	16.983(3)	16.182(8)	14.047(5)
α, deg	90.00	97.572(18)	70.805(5)	82.691(16)	90.00
β, deg	103.576(4)	112.542(17)	75.569(5)	87.388(19)	99.381(12)
γ, deg	90.00	116.508(17)	86.174(6)	74.600(15)	90.00
Volume, Å^3	5182.5(13)	2067(5)	1655.3(5)	1740.0(15)	1461.6(9)
Z	4	2	2	2	4
$D_{\text{calcd.}}$, Mg/m^3	1.307	1.226	1.526	1.387	1.628
μ Mo-Kα, mm^{-1}	0.447	0.482	0.519	0.492	0.121
F(000)	2144	782	788.0	752	736
θ range, deg	1.13– 22.98	2.67 – 20.56	2.32– 23.45	2.15– 22.41	2.35 – 28.01
Reflections	34388	50440	12848	22258	16482
Reflections unique	7096	9134	4065	7289	3615
R(int)	0.0775	0.0795	0.1169	0.0731	0.1428
Data ($I>2\sigma(I)$)	5161	6027	3058	4912	2268
Parameters refined	641	471	490	462	247
Goodness-of-fit on F^2	1.090	0.695	0.986	0.814	1.487
R_1 [$I>2\sigma(I)$]	0.0825	0.0530	0.0672	0.0450	0.0957
wR_2	0.2210	0.1733	0.1641	0.1210	0.2661

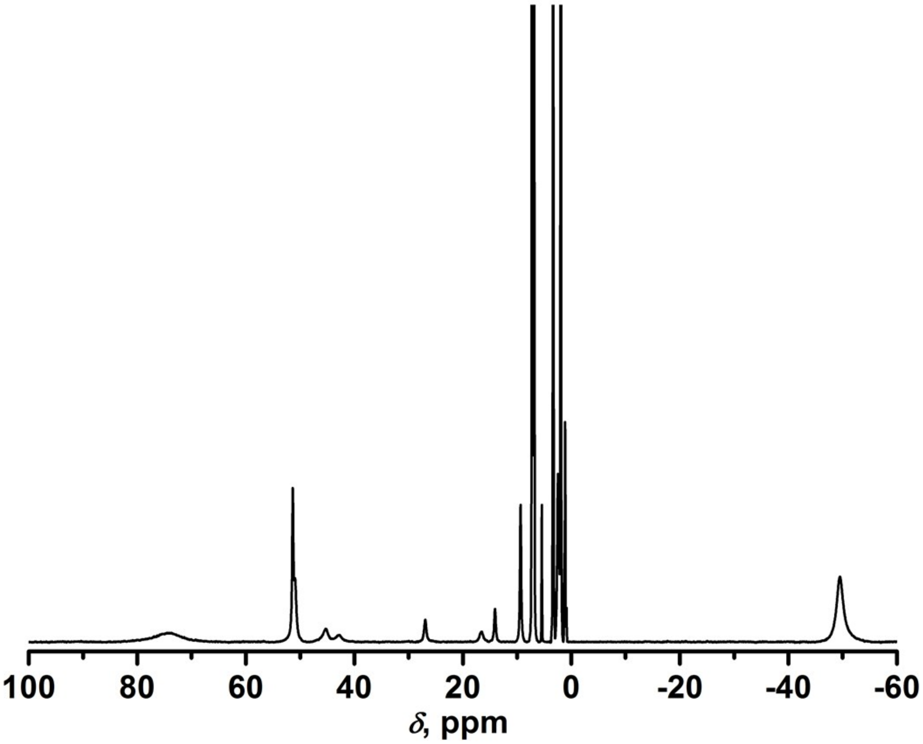

Figure S1. ^{1}H NMR (500 MHz, CD_3CN, 298 K) spectrum of [(6-Me$_3$-TPA)Fe^{II}(GN-H)](BPh_4) (**1**).

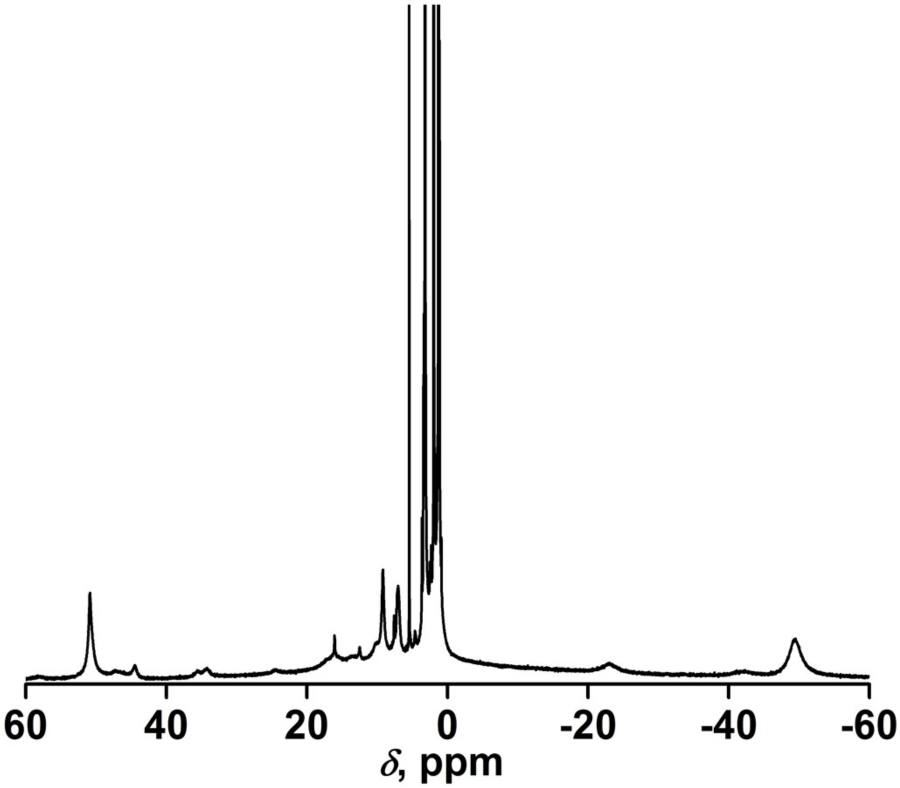

Figure S2. ^{1}H NMR (500 MHz, CD_3CN, 298 K) spectrum of [(6-Me$_3$-TPA)Fe^{II}(DHN-H)](ClO_4) (**1a**).

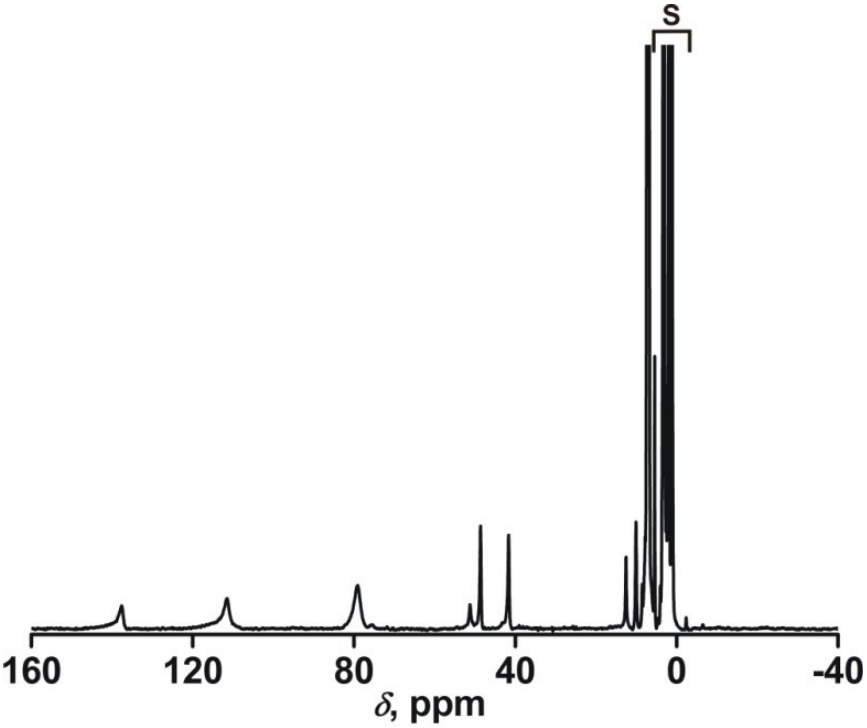

Figure S3. ^{1}H NMR (500 MHz, CD_3CN, 298 K) spectrum of [(BPMEN)Fe^{II}(GN-H)](ClO_4) (**2**). Peaks marked with 'S' originate from residual solvents.

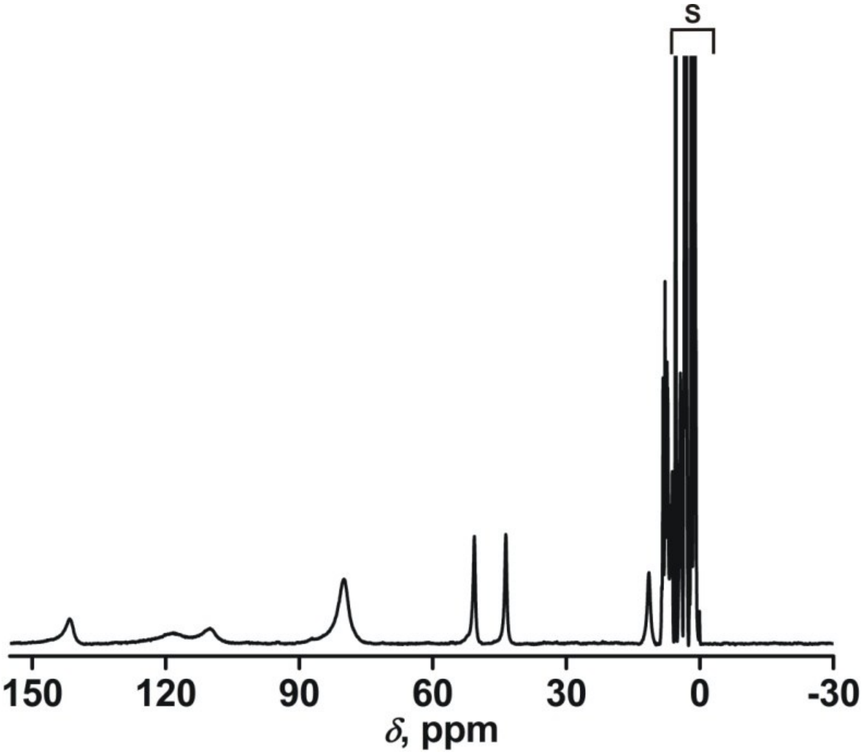

Figure S4. ^{1}H NMR (500 MHz, CD_3CN, 298 K) spectrum of [(BPMEN)Fe^{II}(DHN-H)](ClO_4) (**2a**). Peaks marked with 'S' originate from residual solvents.

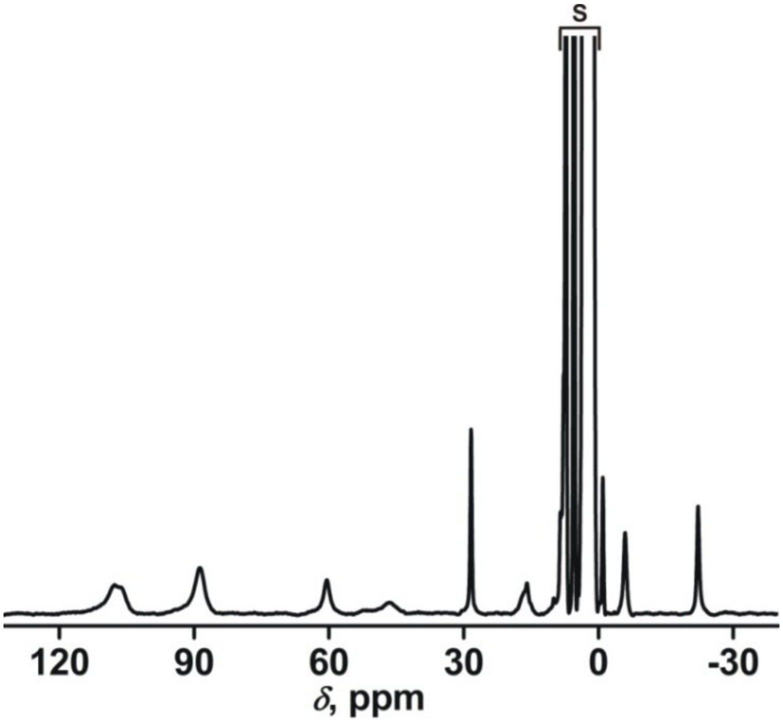

Figure S5. ^{1}H NMR (500 MHz, CD_3CN, 298 K) spectrum of $[(BPMEN)Fe^{II}(HNA)](ClO_4)$ (**2b**). Peaks marked with 'S' originate from residual solvents.

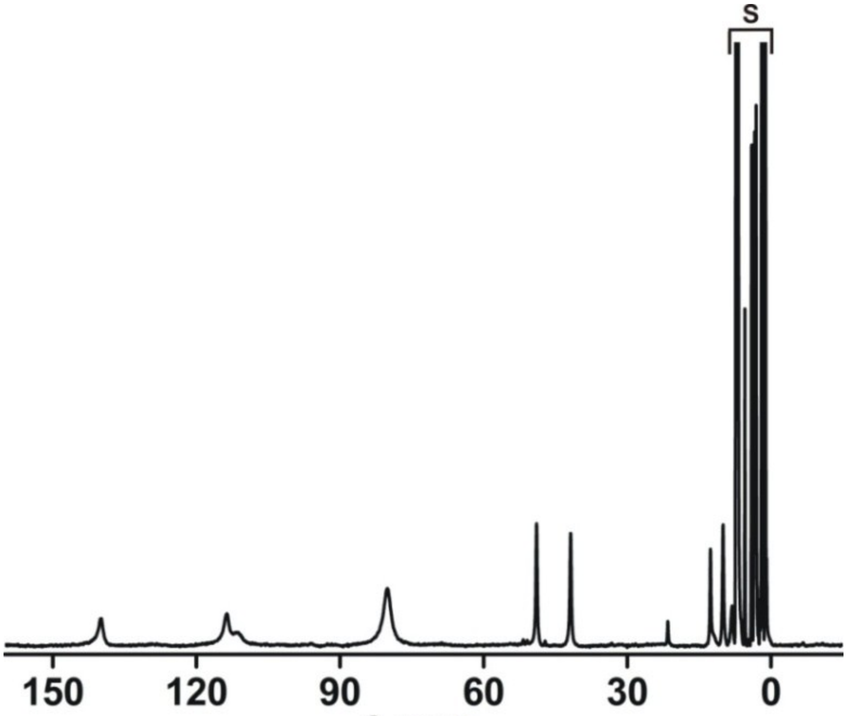

Figure S6. ^{1}H NMR (500 MHz, CD_3CN, 298 K) spectrum of $[(BPMEN)Fe^{II}(5\text{-}OMeSA)](BPh_4)$ (**2c**). Peaks marked with 'S' indicate peaks from residual solvents.

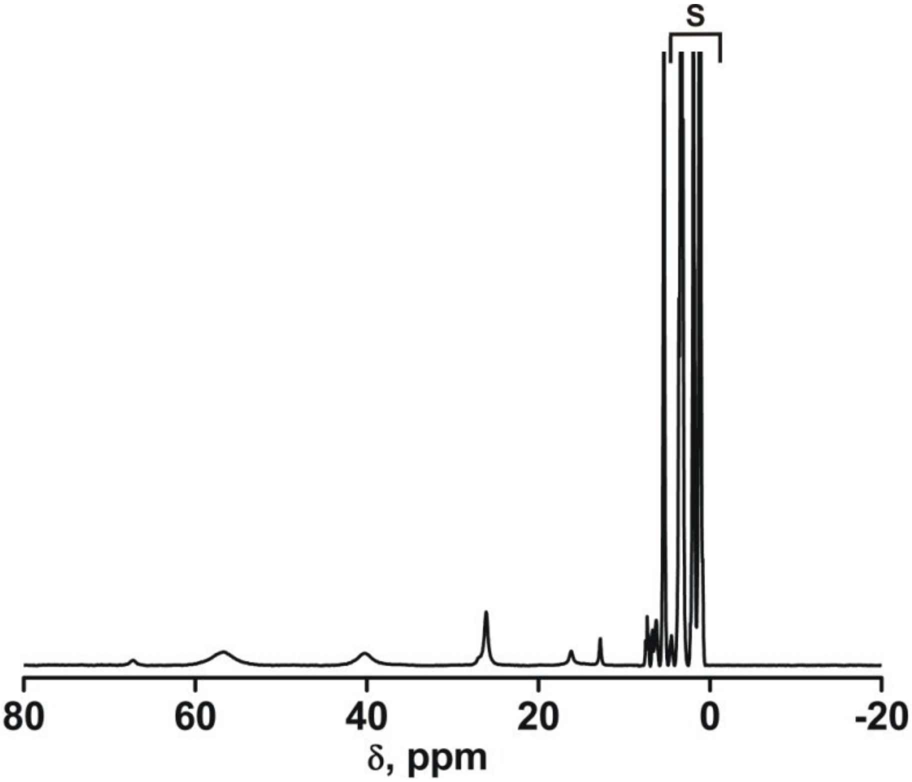

Figure S7. ^{1}H NMR (500 MHz, CD_3CN, 298 K) spectrum of [(TBimA)Fe^{II}(GN-H)](GN-H) (**3**). Peaks marked with 'S' originate from residual solvents.

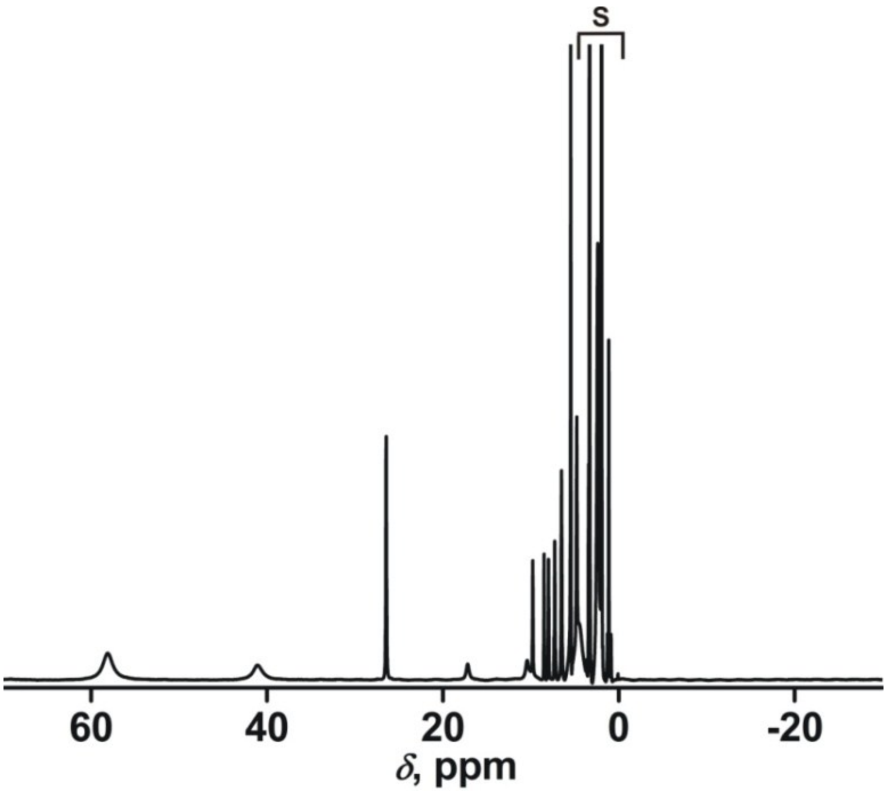

Figure S8. ^{1}H NMR (500 MHz, CD_3CN, 298 K) spectrum of [(TBimA)Fe^{II}(DHN-H)](ClO_4) (**3a**). Peaks marked with 'S' originate from residual solvents.

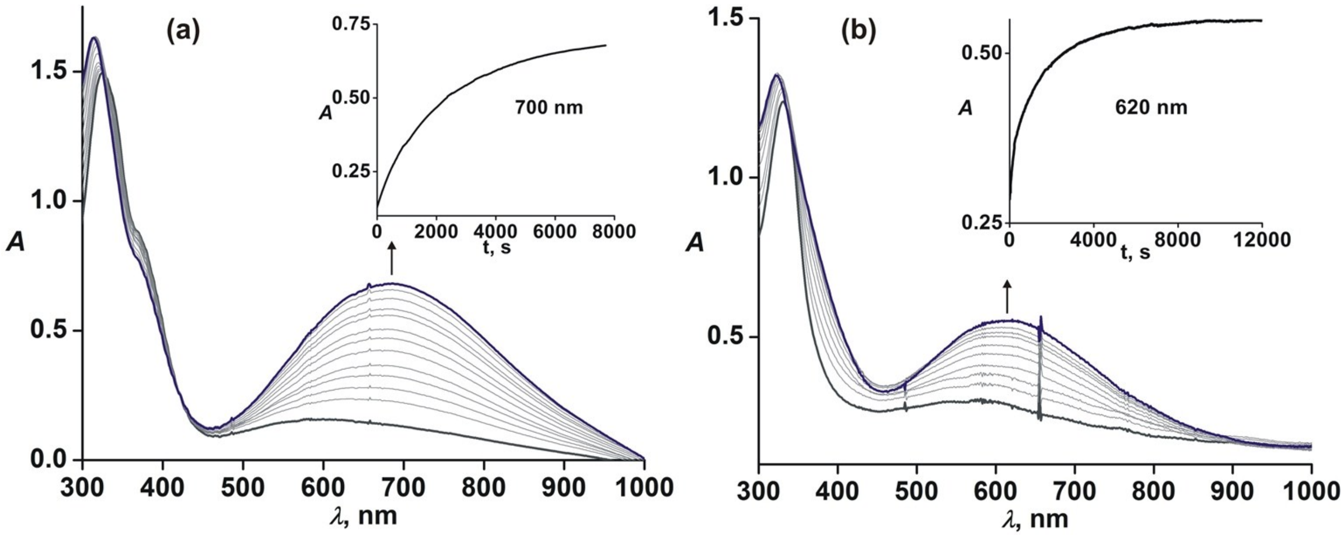

Figure S9. Optical spectral changes of (a) **2** and (b) **3** (0.5 mM in acetonitrile) in the reaction with dioxygen at 298 K. Inset: Plot of absorbance vs time.

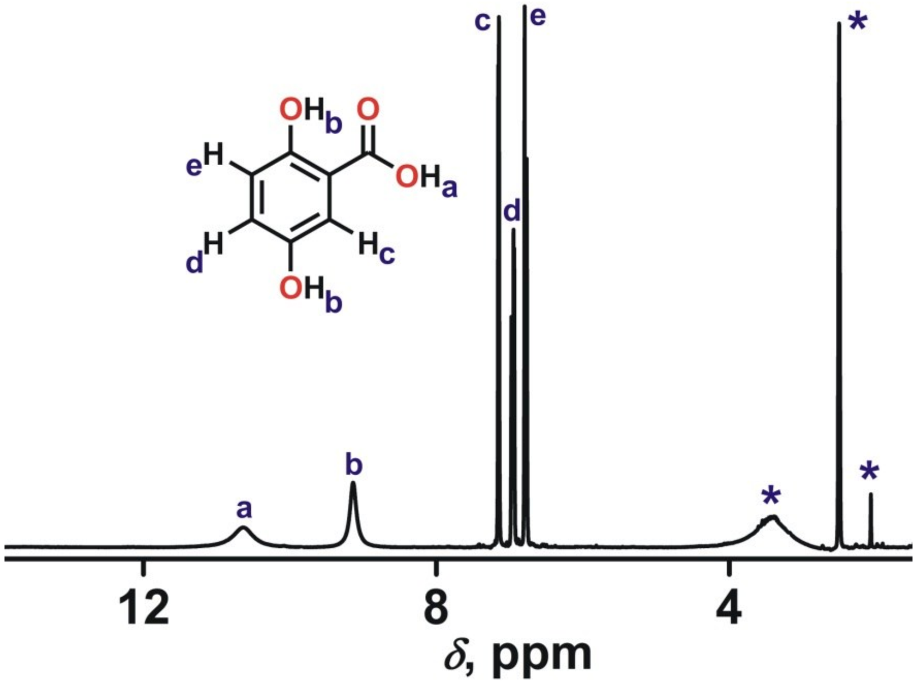

Figure S10. ^{1}H NMR (300 MHz, DMSO$_6$ at 298 K) spectrum of the organic compound isolated from the oxidized solution of **3**. The peak marked with * are from solvents.

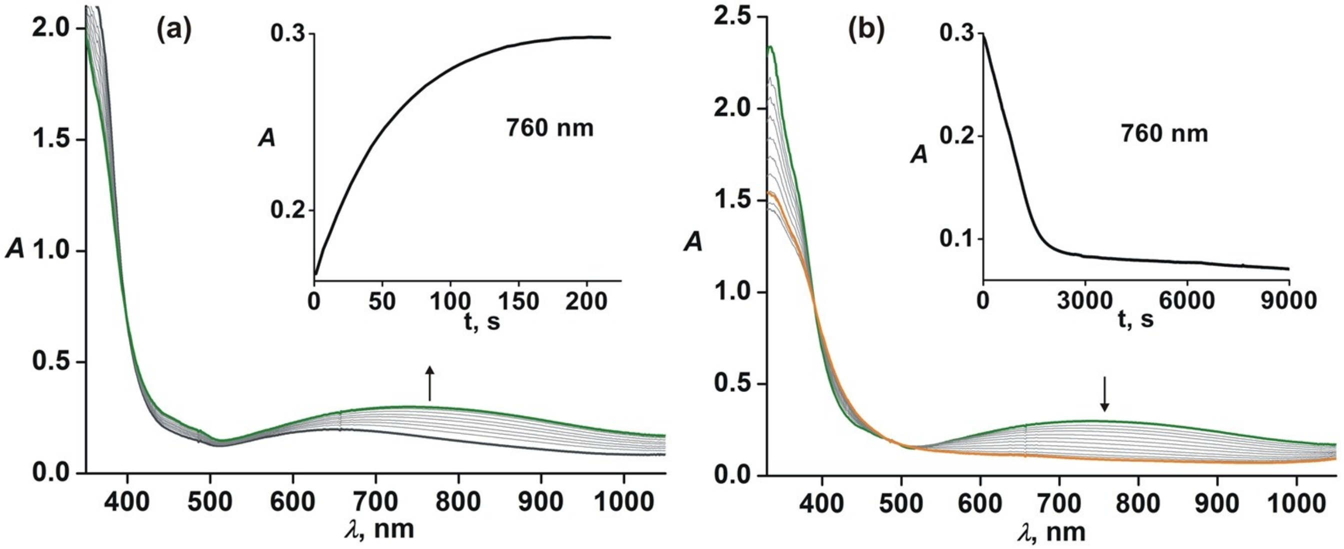

Figure S11. Optical spectral changes of **2a** (0.5 mM in acetonitrile) in the reaction with dioxygen at 298 K. (a) Reaction in the first 3 min and (b) reaction in the next 2 h. Inset: Plot of absorbance vs time.

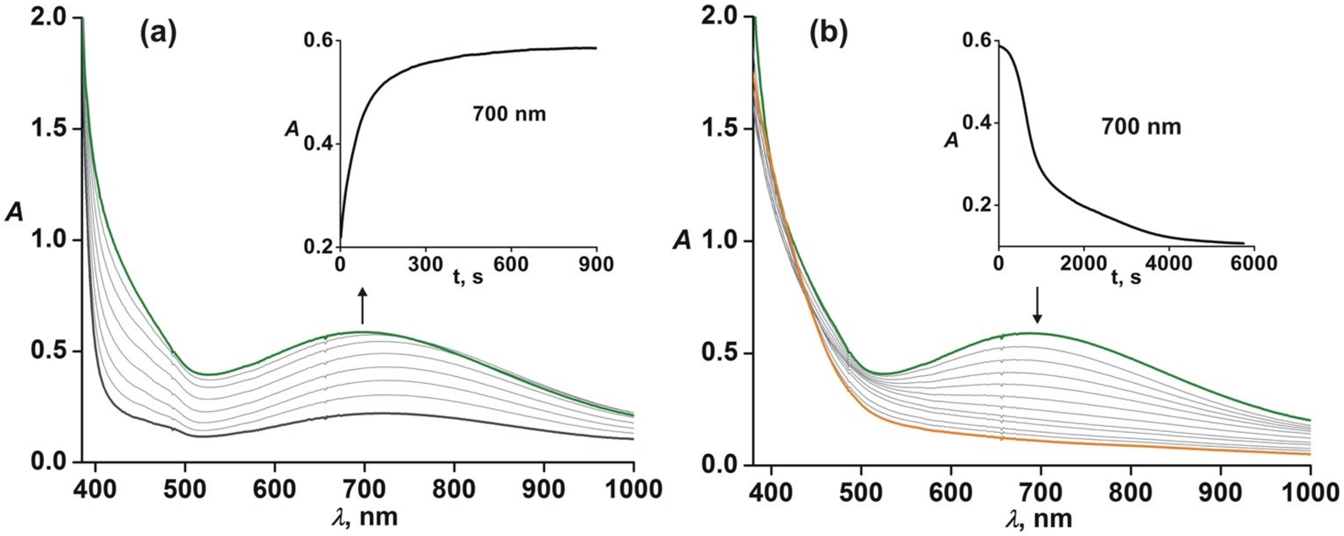

Figure S12. UV-vis spectral change of **3a** (0.5 mM in acetonitrile) upon exposure to dioxygen at 298 K. (a) Reaction in the first 15 min and (b) reaction in the next 1.5 h. Inset: Plot of absorbance vs time.

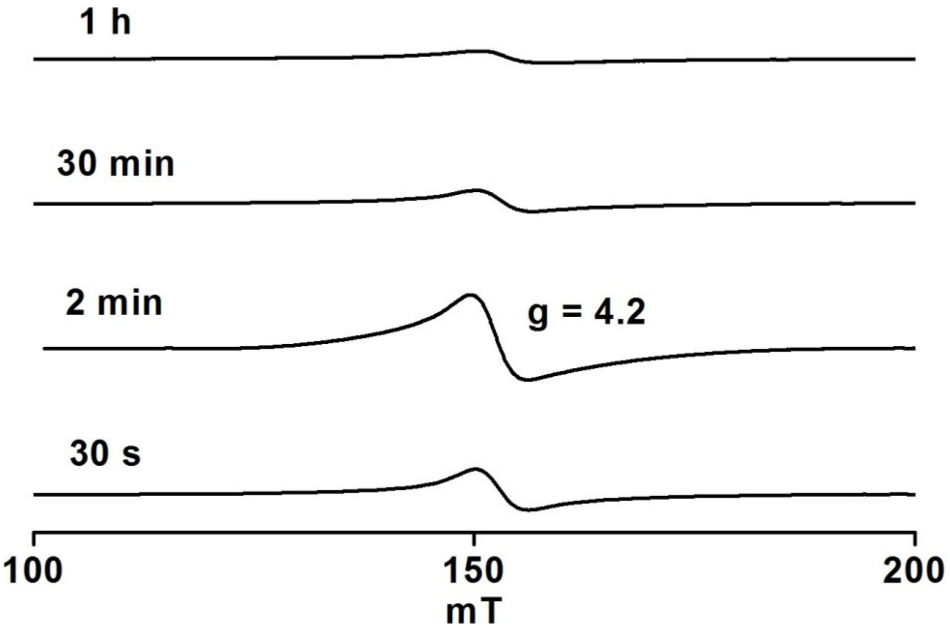

Figure S13. Time dependent X-band EPR spectra (at 77 K) of **2a** during the reaction with dioxygen in acetonitrile. (Experimental conditions for EPR: temperature = 77 K, microwave frequency = 9.12 GHz, microwave power = 10 mW, modulation amplitude = 100 kHz, modulation width = 1.4 mT, time constant = 0.03 s).

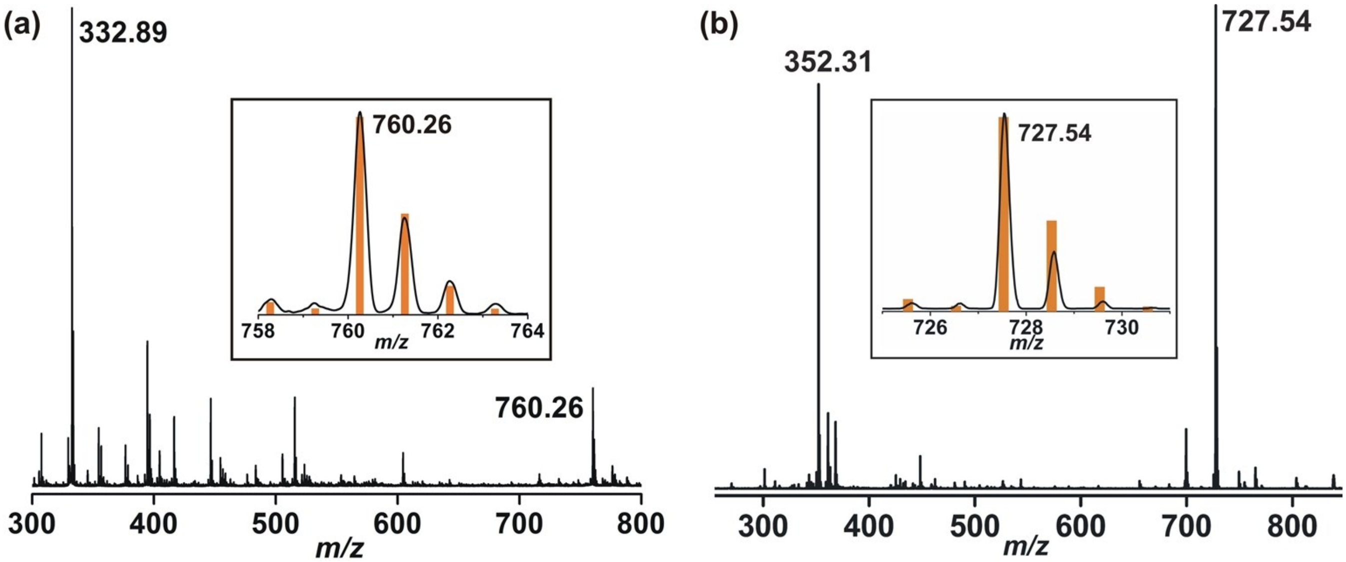

Figure S14. ESI-mass spectrum (positive ion mode in acetonitrile) of the oxidized solution of (a) **1a** and (b) **2a**. Insets: Isotope distribution patterns of the ions peaks.

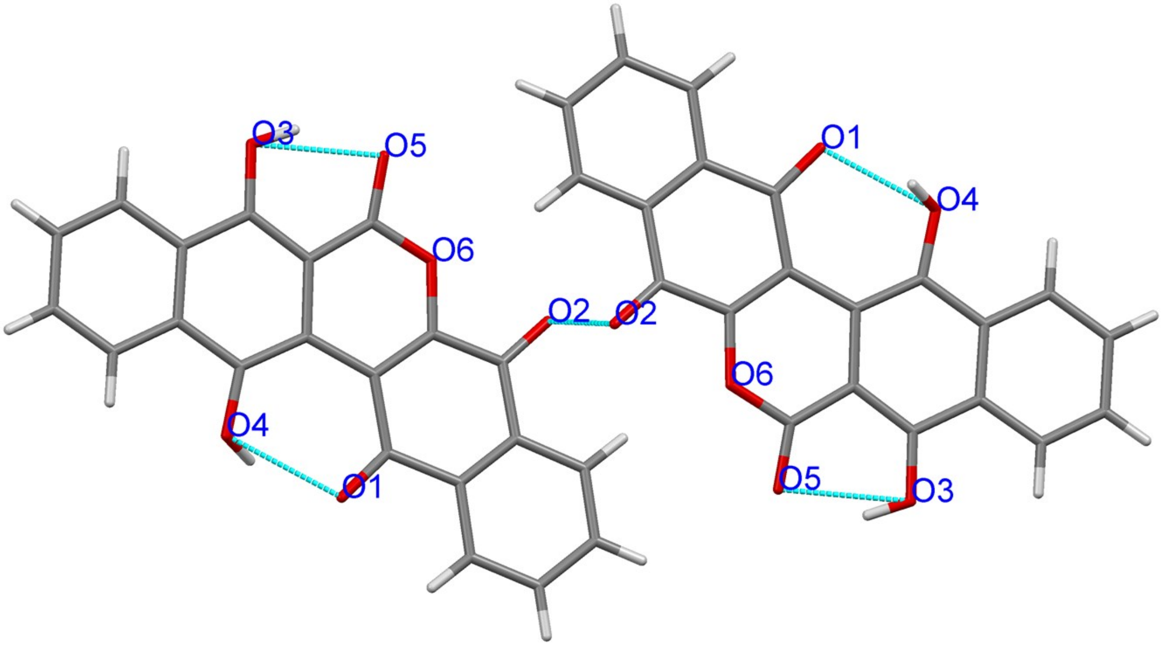

Figure S15. Hydrogen bonding interactions in DNCT (**2F**). The O1...O4 and O3 ....O5 distances are 2.489 Å and 2.542 Å, respectively.

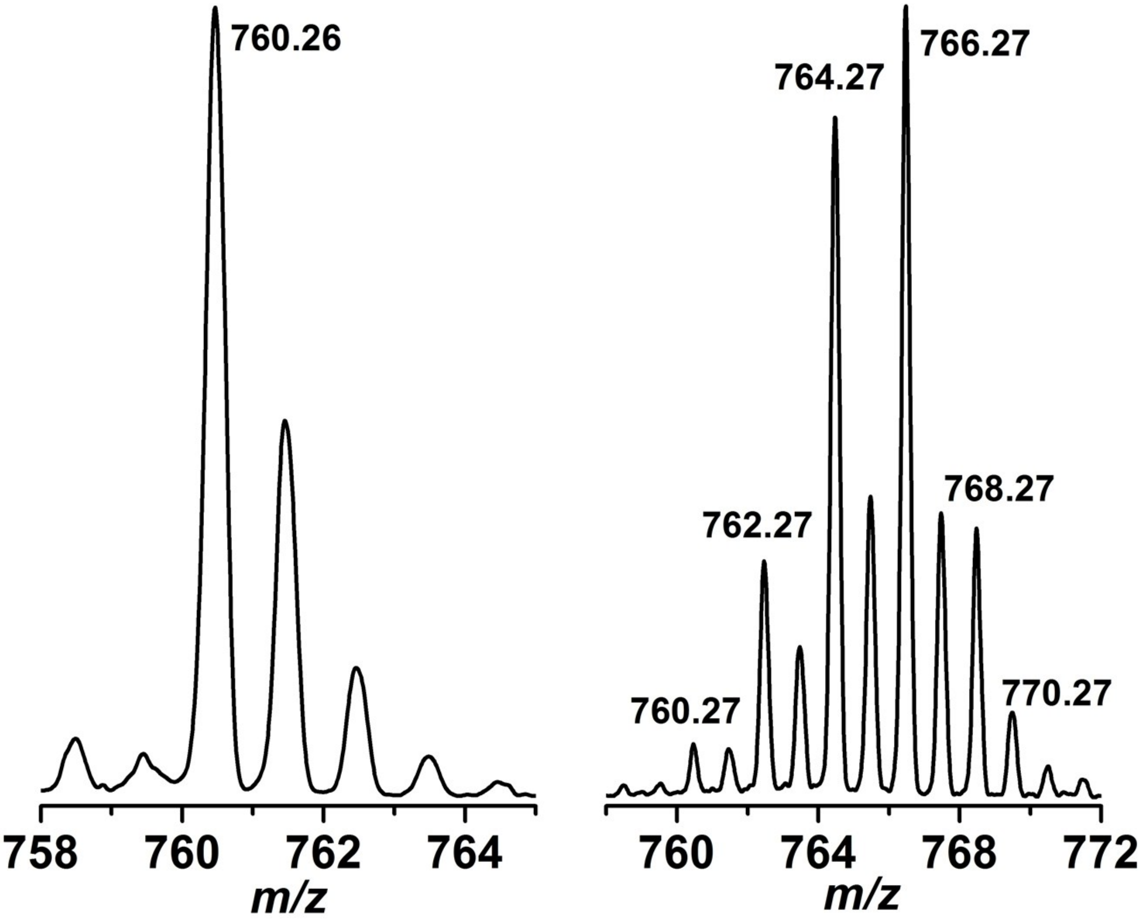

Figure S16. ESI-mass spectrum (positive ion mode in acetonitrile) of the oxidized complex from **1a** in the presence of (a) H_2O and (b)$H_2{}^{18}O$.

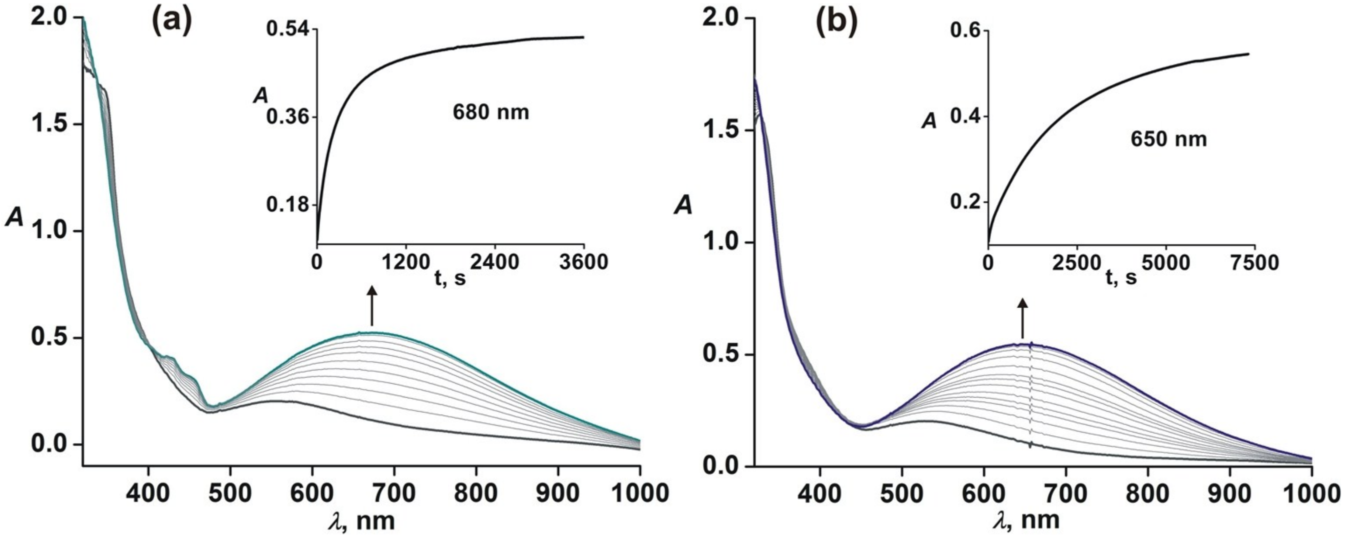

Figure S17. Optical spectral changes of (a) **2b** (b) **2c** (0.5 mM in acetonitrile) in the reaction with dioxygen at 298 K. Inset: Plot of absorbance vs time.

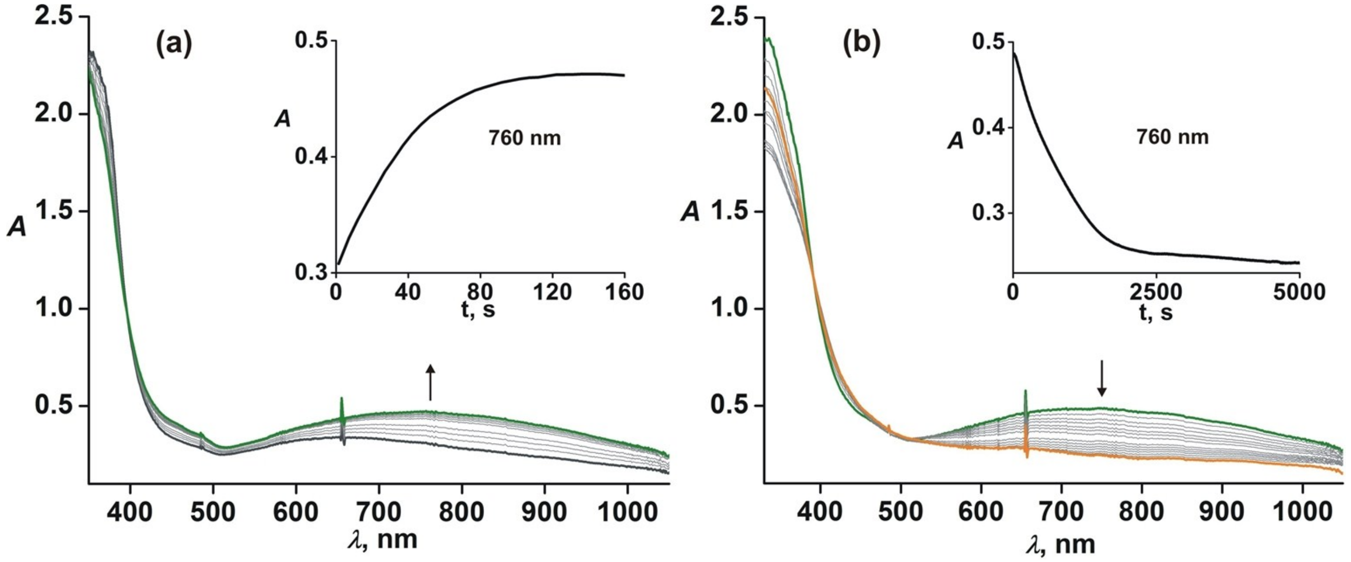

Figure S18. Optical spectral changes of **2a** (0.5 mM in acetonitrile) (a) in the reaction with Ag$^+$ under nitrogen atmosphere; (b) decay of the band after reaction with dioxygen at 298 K. Inset: Plot of absorbance vs time.

……………